The ferroelectric soft mode and central mode in $SrBi_2Ta_2O_9$ films

2003 J. Phys.: Condens. Matter 15 8095

(http://iopscience.iop.org/0953-8984/15/47/012)

INSTITUTE OF PHYSICS PUBLISHING JOURNAL OF PHYSICS: CONDENSED MATTER

J. Phys.: Condens. Matter **15** (2003) 8095–8102 PII: S0953-8984(03)70177-5

The ferroelectric soft mode and central mode in $SrBi_2Ta_2O_9$ films

M Kempa[1], P Kužel[1], S Kamba[1], P Samoukhina[1], J Petzelt[1], A Garg[2] and Z H Barber[2]

[1] Institute of Physics, Academy of Sciences of the Czech Republic, Na Slovance 2, 18221 Prague 8, Czech Republic
[2] Department of Materials Science and Metallurgy, University of Cambridge, Pembroke Street, Cambridge CB2 3QZ, UK

E-mail: kuzelp@fzu.cz

Received 9 October 2003
Published 14 November 2003
Online at stacks.iop.org/JPhysCM/15/8095

Abstract

The dynamics of the ferroelectric phase transition in a $SrBi_2Ta_2O_9$ film of 5.5 μm thickness deposited on sapphire was studied by means of time-domain terahertz transmission spectroscopy (30–300 K) and Fourier transform far-infrared transmission spectroscopy (300–950 K). The optical soft mode near 28 cm^{-1} (at 300 K) exhibits a weak monotonic softening down to 20 cm^{-1} at 950 K with no significant anomaly near either the ferroelectric or ferroelastic phase transition. An additional relaxation process below the phonon frequencies was resolved in the terahertz transmission spectra. The critical slowing down of its relaxation frequency could be responsible for the dielectric anomaly near the ferroelectric transition temperature. This indicates that the ferroelectric transition is predominantly of order–disorder type.

1. Introduction

Ferroelectric (FE) $SrBi_2Ta_2O_9$ (SBT) thin films with so-called Aurivillius perovskite layered structure [1] exhibit excellent polarization fatigue-free behaviour and low coercive fields for polarization switching. For this reason this material (along with $Pb(Zr_{1-x}Ti_x)O_3$) is the most frequently used for producing non-volatile FE memories [2, 3]. The ferroelectricity in SBT was discovered at the beginning of the 1960s [4, 5]. However, until recently, SBT was believed to undergo only one structural phase transition (with T_{c1} near 600 K) from the FE phase with orthorhombic space group $A2_1am$ and two formulae per primitive unit cell ($Z_{prim} = 2$) to the paraelectric (PE) phase with tetragonal structure $I4/mmm$ ($Z_{prim} = 1$) [6–8]. In the mid-1990s Reaney *et al* [9] observed an intermediate phase with $Z_{prim} = 2$ above the FE phase transition in some other Aurivillius compounds: $Bi_4Ti_3O_{12}$, $SrBi_4Ti_4O_{15}$, $SrBi_8Ti_7O_{27}$

and $Sr_2Bi_4Ti_5O_{18}$. These results stimulated a search for a similar intermediate phase in SBT. Hints of the intermediate phase were observed in specific heat and structural measurements [10–13]; however, its space group ($Fmmm$ [11], $Amam$ [12, 13] or $B2cb$ [14]) was under debate. A recent direct observation of ferroelastic domains which disappear above $T_{c2} \cong 770$ K [15] showed that the ferroelastic character of this phase is compatible with the $Amam$ space group. This means that the upper phase transition is improper ferroelastic (with doubling of the primitive unit-cell volume on cooling) and that the lower one is proper ferroelectric (no multiplication of the primitive unit-cell volume with respect to the ferroelastic phase).

The dynamics of the FE phase transition in SBT ceramics has been investigated by Raman scattering [16–18] and Fourier transform infrared (FTIR) reflectivity spectroscopy [15, 19]. An optical soft mode (SM) was observed in both kinds of spectrum below 28 cm^{-1}; however, its temperature behaviour was studied in the FE phase only. The Raman intensity of the SM vanishes near T_{c1} due to the change of selection rules in the PE phase; FTIR reflectivity spectra were obtained only below 568 K. The SM is underdamped and softens from 28 cm^{-1} (at 30 K) to 21 cm^{-1} (at 568 K). However, this partial softening connected with a relatively small increase of the SM contribution to the static permittivity cannot account for a significantly larger anomaly of the low-frequency permittivity observed near T_{c1} [4, 5, 15]. In order to explain this anomaly, the existence of a relaxation process below the phonon frequencies—a central mode (CM)—which should critically slow down near T_{c1} has been proposed [15]. So far, the CM has not been directly observed in microwave or far-infrared spectra; on the other hand, a distinct quasielastic contribution has been reported to appear in the Brillouin scattering data near 10 GHz in the vicinity of the FE phase transition [20].

FTIR spectroscopy and time-domain terahertz transmission spectroscopy (TDTS) for transparent samples are more sensitive and more accurate than FTIR reflectivity for opaque samples. SBT bulk samples are opaque in the far-IR range due to the strong polar lattice vibrations [15]. This was the motivation for our investigation of thin films: to check for the existence of a CM corresponding to the presumed relaxation mechanism and to investigate its temperature dependence. The present work significantly extends the knowledge on the phase transition dynamics in SBT: on one hand, TDTS is a highly sensitive tool for the investigation of polar excitations in the sub-millimetre and millimetre spectral range; on the other hand, our new furnace enabled us to perform FTIR transmission measurements up to 950 K so we were able to investigate the SM behaviour far above both phase transitions.

2. Experimental techniques

We studied three samples at room temperature (RT): an SBT thin film (thickness 0.4 μm) prepared by pulsed laser deposition on a Si substrate (identical to the film studied in [19]), and SBT films (thicknesses 1.5 and 5.5 μm) prepared by pulsed laser deposition on sapphire substrates [21]. As expected, the highest accuracy of the measurements was achieved with the thickest SBT film (5.5 μm), and we have therefore selected it for further, more detailed, temperature studies. We have checked that the parameters of the SM that we have evaluated from the spectra agree within the experimental errors with each other for all three samples. We note also that the Si substrate becomes opaque at high temperatures (above 600 K) in the far-IR range due to the free-carrier absorption, and thus it is not suitable for high-temperature studies. On the other hand, sapphire remains transparent in the far-IR range over the whole temperature range studied.

An Optistat CF cryostat with Mylar windows was used for the cooling down to 30 K (TDTS), and a commercial high-temperature cell SPECAC P/N 5850 was used for heating up to 950 K (FTIR spectrometer).

TDTS measurements were performed using a set-up similar to that described in [22]; the THz spectrometer was powered by an amplified femtosecond laser system (Quantronix, Odin): we used two identical 1 mm [110] ZnTe single crystals to generate (optical rectification) and detect (electro-optic sampling) the THz pulses. The TDTS technique allows determination of the complex dielectric response $\varepsilon^*(\omega)$ of the samples in the range from 6 to 80 cm^{-1} [22]. The experiment consisted of three consecutive measurements for each temperature:

(i) measurement of a signal waveform with the thin film on a substrate in the path of the THz beam,
(ii) measurement of a reference waveform with a bare substrate, and
(iii) measurement of a waveform with an empty sample holder.

The measurements (ii) and (iii) serve for the determination of the dielectric spectrum of the substrate [22]; the measurements (i) and (ii) are used for the characterization of the thin film [23].

FTIR transmission spectra were obtained using a spectrometer, Bruker IFS 113v, equipped with a helium cooled (1.5 K) Si bolometer. Above RT a polyethylene filter was used to reduce the radiation from the sample; nonetheless, the thermal radiation entering the interferometer from the hot sample was taken into account in our evaluation. Similarly to the case of TDTS, spectra of the bare substrate and SBT film on the substrate were determined for each temperature studied. For a given temperature, the transmission spectrum of a bare substrate was first fitted with a sum of harmonic oscillators using Fresnel formulae for coherent transmission of a plane-parallel sample (i.e. taking into account the interference effects) [24]. The resulting parameters of sapphire were then used for the fit of the SBT/sapphire two-layer system. The complex transmittance of the two-layer system was computed by the transfer matrix formalism method including interference effects [25].

3. Results and discussion

The complex dielectric spectra $\varepsilon^*(\omega) = \varepsilon'(\omega) + i\varepsilon''(\omega)$ obtained by means of TDTS measurements for various temperatures were fitted with a sum of two damped Lorentz oscillators (describing the phonons) and a Debye relaxation accounting for the CM:

$$\varepsilon^*(\omega) = \frac{\Delta\varepsilon_r\,\omega_r}{\omega_r + i\omega} + \sum_{j=1}^{2} \frac{\Delta\varepsilon_j\,\omega_j^2}{\omega_j^2 - \omega^2 + i\omega\gamma_j} + \varepsilon_\infty. \tag{1}$$

ω_r and $\Delta\varepsilon_r$ are the relaxation frequency and dielectric strength of the CM, respectively. ω_j, γ_j, and $\Delta\varepsilon_j$ denote the eigenfrequencies, dampings, and contribution to the static permittivity from the jth polar phonon mode, respectively, and ε_∞ describes the high-frequency permittivity originating from the electronic polarization and from polar phonons above the spectral range studied. Typical examples of the dielectric response obtained from the TDTS experiment in the cryostat are depicted in figure 1; a decomposition of the dielectric spectrum into the components is shown for the temperature 270 K. The changes versus temperature of a low-frequency feature interpreted as a CM can be clearly identified in the plot of the imaginary part of the permittivity. It is worth pointing out that the measured data do not obey exactly the Kramers–Kronig relations for the lowest frequency range (below 10 cm^{-1}): the low-frequency part of the measured $\varepsilon'(\omega)$ is slightly underestimated and shows a small decrease instead of the increase required by the Kramers–Kronig analysis of $\varepsilon''(\omega)$. The real part of the permittivity is mainly related to the phase of the THz pulse transmitted through the sample and it has been shown that this phase may exhibit a large experimental error in the measurements with

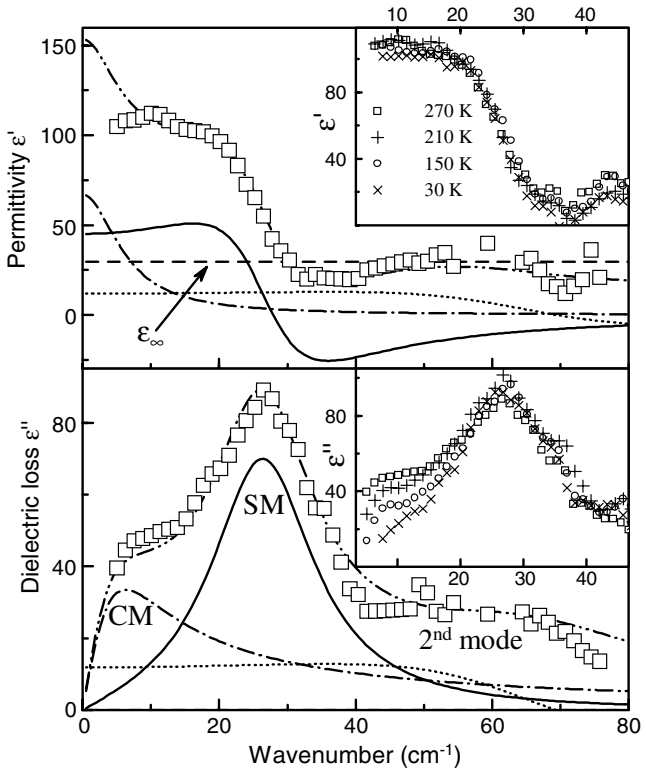

Figure 1. The complex dielectric function of SBT film obtained by means of a TDTS at 270 K (film thickness 5.5 μm). The resulting fit and its components are shown (see the text). Insets: changes of the complex dielectric function with temperature.

thin films [23]. On the other hand, a monotonic increase of $\varepsilon'(\omega)$ has been observed in the measurement at RT without the cryostat. We thus concluded that this effect is predominantly due to a phase error of the measurements in the cryostat and we did not take it into account during the fitting procedure.

One can see from figure 1 that the contribution of all polar phonons to the static permittivity is only about 100, although it is well known that the low-frequency permittivity is usually higher than 150 at RT [4, 5, 26]. We note that the thickness dependence of ε' in SBT thin film was observed only below 200 nm [26], which is much less than the 5.5 μm that we used. Therefore we assume that the permittivity of our film agrees with that of the bulk samples. The CM improves the fit below 20 cm^{-1} and its presence explains the missing permittivity. The parameters of the CM and their variation with temperature below RT are shown in figure 2. The relaxation frequency ω_r distinctly softens while the contribution of the relaxation to the static permittivity $\Delta\varepsilon_r$ increases upon heating. Unfortunately, our THz spectrometer had not then been adapted for high-temperature measurements; therefore the CM properties were evaluated only below RT. A linear fit of ω_r according to the classical law $\omega_r = A(T_{cr} - T)$ gives $T_{cr} = 350 \pm 25$ K (see the dotted curve in figure 2). As the dielectric strength of the CM is very low below 140 K, the accuracy of the evaluation of ω_r is limited (see the error bars in figure 2). If the linear fit is performed only using the more accurate data taken above 140 K (see the dashed curve in figure 2), the critical temperature is found to be 510 ± 40 K, which is significantly closer to T_{c1}. We note also that T_{c1} is strongly dependent on the stoichiometry

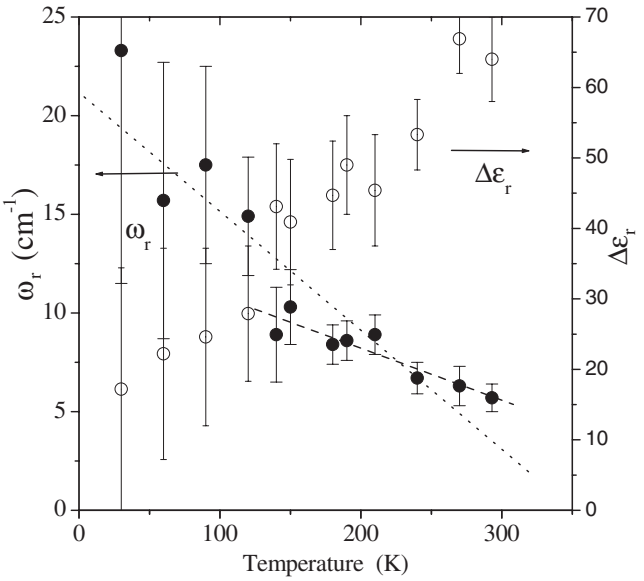

Figure 2. The temperature dependence of the CM frequency ω_r and its dielectric strength $\Delta\varepsilon_r$. Results of two kinds of linear fit of $\omega_r(T)$ are also shown (see the text).

of the SBT sample [8, 27] and that the strain in the film can also influence its value. From recent micro-Brillouin scattering data it is known that the CM reaches a frequency of 8 GHz at 560 K [20].

The lowest-frequency polar phonon (denoted as SM similarly to in [15]) slightly softens from 28.5 cm^{-1} (at 30 K) to 26.5 cm^{-1} (at RT), which agrees with the results of IR reflectivity studies of bulk ceramics within the accuracy of the experiment [15]. Our RT spectrum corresponds also to the recently published THz spectrum of SBT thin film on MgO substrate [28]; however, the temperature dependence was not studied there.

The SM behaviour above RT was investigated by means of FTIR transmission spectroscopy (see figure 3). The sample was semi-transparent below 170 cm^{-1} at RT, but the transmission decreased on heating. The upper limit of the transparency decreased to 100 cm^{-1} at 950 K: this still allowed us to evaluate the temperature dependences of the two lowest-frequency polar phonons. Oscillations in the transmission spectra correspond to interference within the sapphire substrate; broad minima are due to the phonon absorption bands of the SBT film.

High-temperature complex dielectric functions of the SBT film obtained from the fits are shown in figure 4. The effect of the SM softening is clearly seen: the dielectric loss peak (approximately the SM frequency) shifts to lower frequencies and the low-frequency permittivity increases on heating. The SM contribution to the static permittivity ($\Delta\varepsilon_{SM}$) exhibits a monotonic increase from 60 at RT up to 140 at 950 K (see figure 5). Notice the slight change of the slope of $\Delta\varepsilon_{SM}(T)$ near T_{c1} and $\omega^2_{SM}(T)$ near T_{c2}: this indicates that the SM is influenced by both phase transitions. However, the SM does not drive the phase transitions in SBT since no signs of hardening were observed in ω_{SM} above T_{c1}. The CM was not considered in our FTIR fits because of the limited experimental accuracy below 20 cm^{-1}. We expect the absence of the CM contribution in our fits to be responsible for the difference between the low-frequency permittivity obtained from our fits (see figure 4) and the experimental values near T_{c1} ($\varepsilon_{max} = 300$–550). The relaxational CM detected in the THz spectra thus seems to be

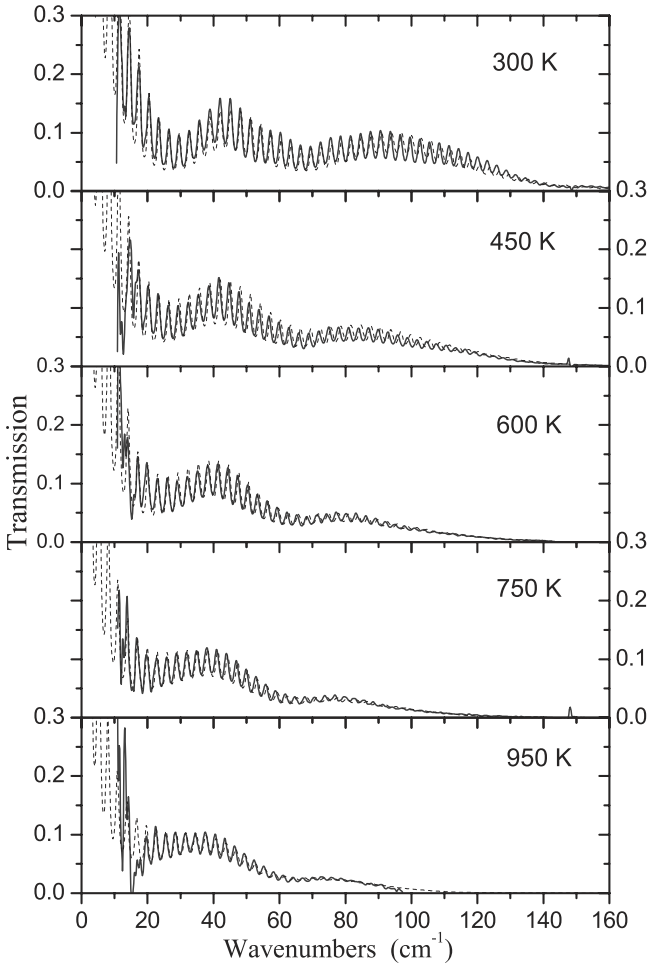

Figure 3. The FTIR transmission of SBT thick film on a sapphire substrate plotted at selected temperatures. Solid curves are experimental spectra; dashed lines are results of the fit. Substrate thickness 544 μm; film thickness 5.5 μm.

the driving force of the FE phase transition: the phase transition is therefore prevailingly of order–disorder type.

Let us discuss the assignment of observed excitations. It is known that the displacement of Sr atoms leads to a cooperative tilting and rotation of the TaO_6 octahedra below T_{c1}. At the same time, Ta atoms shift from the centre of oxygen octahedra [13]. Moreover, there exists a significant concentration of anti-site defects: Macquart *et al* [29] reported that in stoichiometric samples 7% of Sr sites are occupied by Bi atoms and vice versa. In non-stoichiometric $Sr_{0.8}Bi_{2.2}Ta_2O_9$ the Bi excess atoms are at Sr sites, which leads to an increase of the remanent polarization and of T_{c1} [8]. Bi ions are smaller than Sr ions so the Bi ions may occupy off-centre positions at Sr sites and thus may be dynamically disordered. The observed CM may then be assigned to anharmonic vibrations of Bi ions at the Sr sites. Vibrations of atoms at Sr sites are coupled with the vibrations of TaO_6 octahedra (SM) and can possibly influence their softening. The hard mode near 60 cm^{-1} has the symmetry B_1 (i.e. it is active in $E \parallel c$ spectra) since it was not observed in FTIR reflectivity spectra of (001) oriented

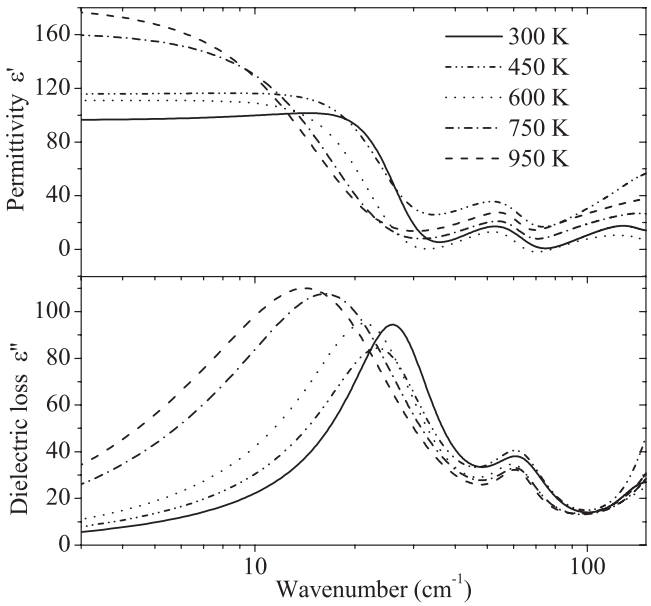

Figure 4. The complex dielectric function obtained from FTIR transmission spectra at selected temperatures.

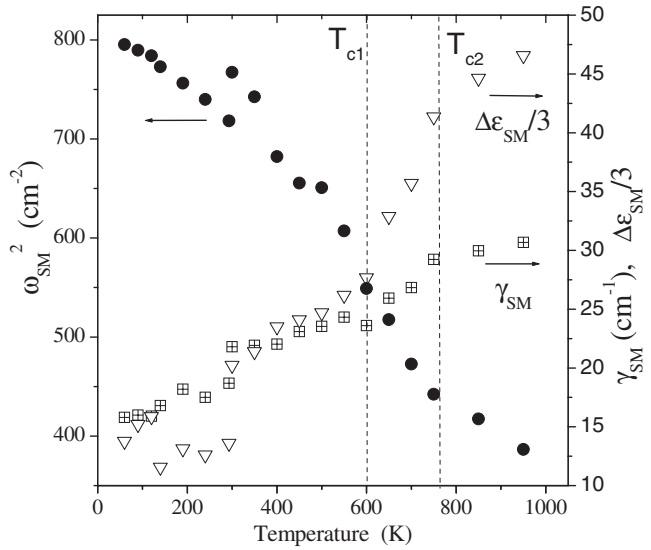

Figure 5. The temperature dependence of the squared SM frequency ω_{SM}^2, of the SM damping γ_{SM}, and of dielectric strength $\Delta\varepsilon_{SM}$ obtained from the fits of the TDT (below RT: TDTS data, above RT: FTIR data). The steps at RT are partly due to the experimental errors, and partly due to different fitting functions (with and without the CM) used below and above RT, respectively.

single-crystal SBT [15] and can be assigned to the Bi displacements in Bi_2O_2 layers [17]. The SM is of A_1 symmetry (vibrations along the FE **a** axis) and therefore cannot bilinearly couple with the B_1 mode.

4. Conclusions

We can summarize by saying that the SM frequency exhibits a monotonic decrease in the temperature range 20–950 K. The dielectric anomaly near T_{c1} should be caused by a critical slowing down of the CM which was revealed below RT by means of TDTS. High-temperature TDTS measurements are needed for a more detailed study of the CM behaviour near T_{c1}. This experiment is in progress.

Acknowledgments

The work was supported by the Grant Agency of the Czech Republic (project Nos 202/01/0612 and 202/02/0238), Academy of Sciences (project No A1010213) and the Ministry of Education of the Czech Republic (project No LN00A032).

References

[1] Aurivillius B 1949 *Ark. Kemi* **1** 463
Aurivillius B 1949 *Ark. Kemi* **1** 499
Aurivillius B 1950 *Ark. Kemi* **2** 519
Aurivillius B 1952 *Ark. Kemi* **5** 39
[2] Paz de Araujo C A, Cuchiaro J E, McMillan L D, Scott M C and Scott J F 1995 *Nature* **374** 627
[3] Scott J F 1998 *Ferroelectr. Rev.* **1** 1
[4] Smolenskii G A, Isupov V A and Agranovskaya A I 1961 *Sov. Phys.—Solid State* **3** 651
[5] Subbarao E C 1962 *J. Phys. Chem. Solids* **23** 665
[6] Newnham R E, Wolfe R W, Horsey R S, Diaz-Colon F A and Kay M I 1973 *Mater. Res. Bull.* **8** 1183
[7] Rae A D, Thompson J G and Withers R L 1992 *Acta Crystallogr.* B **48** 418
[8] Shimakawa Y, Kubo Y, Nakagawa Y, Kamiyama T, Asano H and Izumi F 1999 *Appl. Phys. Lett.* **74** 1904
[9] Reaney I M, Roulin M, Shulman H S and Setter N 1995 *Ferroelectrics* **165** 295
[10] Onodera A, Yoshio K, Myint C C, Kojima S, Yamashita H and Takama T 1999 *Japan. J. Appl. Phys.* **38** 5683
[11] Onodera A, Kubo T, Yoshio K, Kojima S and Yamashita H 2000 *Japan. J. Appl. Phys.* **39** 5711
[12] Hervoches C H, Irvine J T S and Lightfoot P 2001 *Phys. Rev.* B **64** 100102
[13] Macquart R, Kennedy B J, Hunter B A, Howard C J and Shimakawa Y 2002 *Integr. Ferroelectr.* **44** 101
[14] Kim J S, Cheon C, Shim H-S and Lee C L 2001 *J. Eur. Ceram. Soc.* **21** 1295
[15] Kamba S, Pokorný J, Porokhonskyy V, Petzelt J, Moret M P, Garg A, Barber Z H and Zallen R 2002 *Appl. Phys. Lett.* **81** 1056
[16] Kojima S 1998 *J. Phys.: Condens. Matter* **10** L327
[17] Kojima S and Saitoh I 1999 *Physica* B **263/264** 653
[18] Ching-Prado E, Pérez W, Reynés-Figueroa A, Katiyar R S and Desu S B 1999 *Ferroelectr. Lett.* **25** 53
[19] Moret M P, Zallen R, Newnham R E, Joshi P and Desu S B 1998 *Phys. Rev.* B **57** 5715
[20] Ko J-H, Hushur A and Kojima S 2002 *Appl. Phys. Lett.* **81** 4043
[21] Garg A and Barber Z H 2002 *Ferroelectrics* **268** 509
[22] Kužel P and Petzelt J 2000 *Ferroelectrics* **239** 949
[23] Petzelt J, Kužel P, Rychetský I, Pashkin A and Ostapchuk T 2003 *Ferroelectrics* **288** 169
[24] Born M and Wolf E 1960 *Principles of Optics* (Oxford: Pergamon)
[25] Heavens O S 1960 *Rep. Prog. Phys.* **22** 1
[26] Park J D, Kim J W and Oh T S 2001 *Ferroelectrics* **260** 635
[27] Noguchi Y, Miyayama M and Kudo T 2001 *Phys. Rev.* B **63** 214102
[28] Kawayama I, Kotani K and Tonouchi M 2002 *Japan. J. Appl. Phys.* **41** 6803
[29] Macquart R, Kennedy B J, Kubota Y, Nishibori E and Takata M 2000 *Ferroelectrics* **248** 27